THE JOURNAL OF PHYSICAL CHEMISTRY C

ARTICLE

pubs.acs.org/JPCC

Cyclic Supersaturation and Triple Phase Boundary Dynamics in Germanium Nanowire Growth

A. D. Gamalski,[†] C. Ducati,[‡] and S. Hofmann*,[†]

[†]Department of Engineering, University of Cambridge, Cambridge CB3 0FA, U.K.

[‡]Department of Materials Science and Metallurgy, University of Cambridge, Cambridge CB2 3QZ, U.K.

Supporting Information

ABSTRACT: Video-rate environmental transmission electron microscopy of Au-catalyzed chemical vapor deposition of Ge nanowires shows that growth kinetics are linked to an oscillatory behavior at the liquid−solid interface near the triple phase boundary (TPB), where the nanowire surface consists of an oblique facet. A nanowire growth cycle starts by preferential Ge precipitation at the TPB, which increases the wetting angle and Ge supersaturation of the liquid AuGe catalyst. With a continuously rising Ge supersaturation, the kinetic barrier for Ge bilayer nucleation falls until step nucleation occurs. Subsequent step flow creates a (111)-type plane at the nanowire growth front and hence rapidly decreases the Ge supersaturation in the catalyst. This leads to the destabilization and partial dissolution of the Ge initially stored in the rough TPB area, i.e., completes the growth cycle. The results and arguments are general and based on few system specific assumptions, therefore may be applicable to other nanowire systems, and are relevant to general nucleation and liquid−solid interface dynamics in dimensionally confined systems.

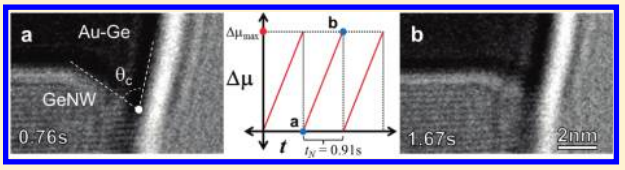

1. INTRODUCTION

Bottom-up nanowire (NW) growth offers unique opportunities for nanoscale device engineering with applications in photonics, sensors, and energy storage.[1,2] Unidirectional NW growth is based on preferential interface nucleation. The widely cited vapor−liquid−solid (VLS) model[3] refers to a three phase system where material supplied from a vapor absorbs into a liquid catalyst alloy and precipitates upon supersaturation to form a solid crystal. A NW then grows in layer-by-layer fashion via the repeated nucleation of steps and their lateral propagation at the liquid−solid catalyst−NW interface.[4] Although such interface dynamics are of key importance to NW growth kinetics, NW crystal structure, and the interface sharpness in NW heterostructures,[5,6] their understanding remains incomplete. The NW−catalyst−vapor triple phase boundary (TPB) is of particular interest in the VLS mechanism as the chemical potential of the growth species can locally vary dependent on the wetting angle,[7] which depends on the surface energies.[8,9] Further, the material incorporation for compound NWs has been suggested to critically depend on the TPB configuration.[10]

Here we present a video-rate lattice-resolved environmental transmission electron microscopy (ETEM) study of interface dynamics during Au- catalyzed chemical vapor deposition (CVD) of Ge NWs. We find that the frequency of Ge bilayer formation at the catalyst/NW interface of ⟨111⟩-oriented Ge NWs is linked to an oscillatory behavior of oblique NW facets near the TPB. We suggest that a growth cycle for a Ge bilayer starts by preferential Ge precipitation at the atomically rough TPB area, which increases the wetting angle of the liquid AuGe catalyst and, via the tension at the TPB, increases the Ge supersaturation in the catalyst. With a continuously rising Ge supersaturation, the kinetic barrier for Ge bilayer nucleation falls until step nucleation occurs. Subsequent step flow rapidly decreases the Ge supersaturation in the catalyst which leads to the destabilization and partial dissolution of the Ge initially stored in the rough TPB area, i.e., completes the growth cycle. Our results and arguments are general and based on few system specific assumptions, therefore may be applicable to other NW systems, and are relevant to general nucleation and liquid−solid interface dynamics in dimensionally confined systems.

2. EXPERIMENTAL METHODS

Figure 1 shows a series of bright field ETEM images of the AuGe catalyst interface around the TPB of a growing Ge NW at ≈310 °C in Ge_2H_6 (30% in He) at ≈4 × 10^{-3} mbar total pressure. We use a modified FEI Tecnai F20 ETEM, operated at 200 kV, equipped with a differential pumping system. Digital video sequences were recorded at 9 frames s^{-1} time resolution using a Gatan Orius 600 camera. Temperatures are measured by a thermocouple on the TEM holder minifurnace. The electron impingement rate was representative of that typically implemented for high-resolution imaging, and the electron beam was never focused on the specimen in order to minimize the effects of electron-beam-induced damage/gas dissociation[11] and sample modifications. Au catalyst particles were prepared by thermal evaporation (nominal Au thickness <2 nm) onto 2000 mesh Cu TEM grids coated with a holey carbon film and a ∼30 nm sputtered SiO_x layer or

Received: October 6, 2010
Revised: February 1, 2011
Published: March 03, 2011

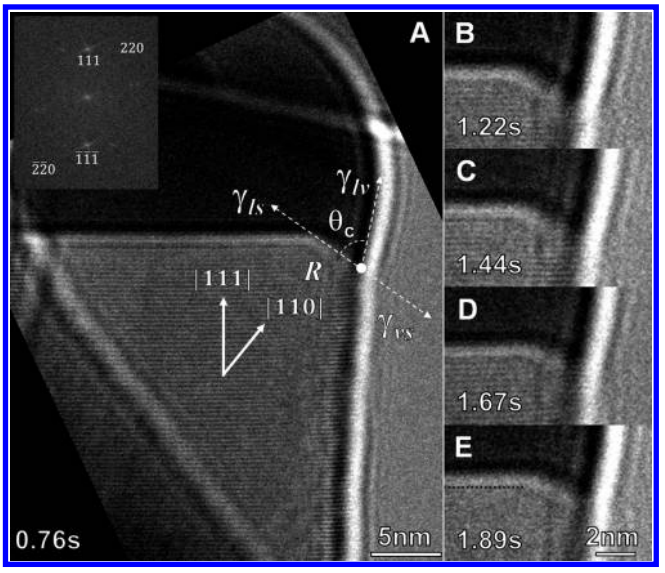

Figure 1. Bright field ETEM image sequence of the catalyst interface around the TPB of a growing Ge NW at ≈310 °C in Ge_2H_6 (30% in He) at ≈4×10^{-3} mbar total pressure (extracted from Supporting Information video S1). The times indicated in (A)−(E) correspond to video S1 and Figure 2. In (A) the atomically rough surface is denoted by *R*, the wetting angle by θ_c, and γ_{lv}, γ_{ls}, and γ_{vs} are the surface energy differences between the liquid−vapor, liquid−solid, and vapor−solid surfaces, respectively. The inset shows a selected area FFT of the Ge NW. In (E) the original (111) solid−liquid interface is traced with a dotted black line to highlight the advancement of the growth interface.

perforated SiO_2 membranes. After preparation, the samples were transferred in air to the ETEM. Although the growth temperature is below the AuGe eutectic temperature T_e = 361 °C, the large kinetic barrier for NW nucleation causes a metastable liquid alloy to form.[12]

3. RESULTS

Figures 1A−E capture one growth cycle for a NW layer, representative of the oscillatory growth behavior we observe by video-rate ETEM (see Supporting Information video S1). The NW grows along a ⟨111⟩ direction and is approximately 27 nm in diameter. The TPB lags behind the (111) growth front by 1−3 nm, being located at the edge of an oblique facet marked as *R*. At the beginning of the cycle (Figure 1A), the angle between the (111) growth plane and *R* is about 35°, indicating that *R* is initially a Ge(110) facet. Figures 1B−D show that Ge precipitates from the liquid AuGe catalyst, attaching preferentially to *R*. Ge precipitation onto *R* decreases both *R*'s projected length and its angle to the (111) growth plane. At the same time, the wetting angle θ_c between *R* and the liquid/vapor interface increases (Figures 1A−D). After step nucleation (Figure 1E), the solid Ge deposited on *R* partially dissolves back into the liquid catalyst and the NW length *L* increases by the height of a single (occasionally double) bilayer. The wetting angle θ_c decreases, and *R* can again be identified with a (110) facet. After the formation of a new Ge bilayer, the process begins anew with the contact angle rising again and Ge precipitating onto *R*.

This oscillatory behavior is captured in Figure 2 where the measured values for the wetting angle θ_c, the unfilled area *A* around *R* at the TPB (as defined by the schematic), and relative length *L* of the NW are plotted. Vertical black dotted lines indicate times when a new Ge bilayer was observed, as measured by a stepped increase in *L*. We note that step-flow itself is too

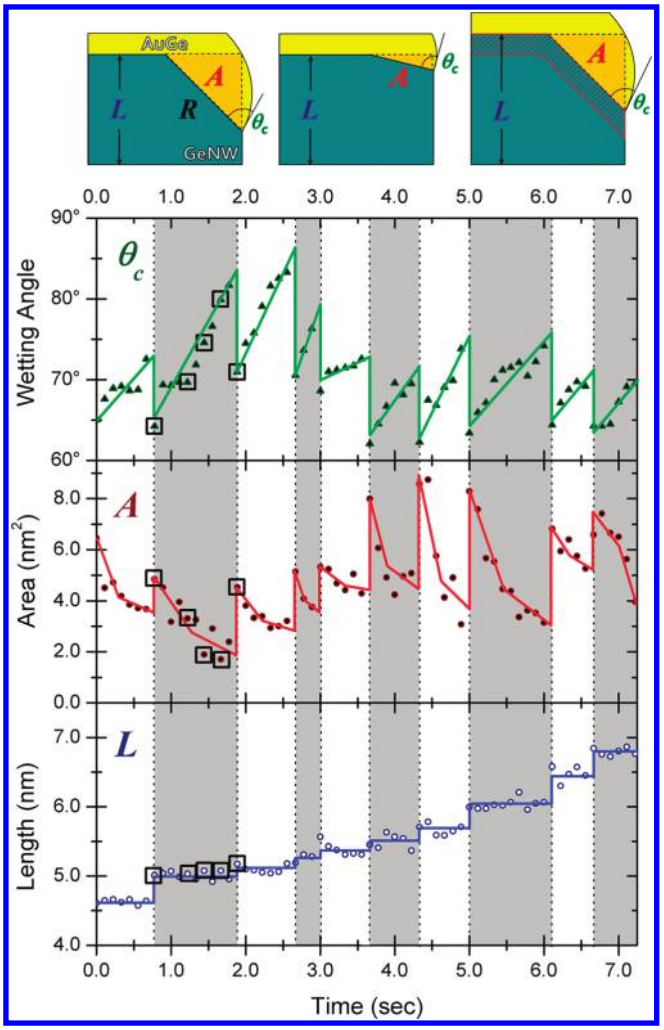

Figure 2. Time dependence of relative NW length *L*, unfilled area *A*, and wetting angle θ_c as measured from video S1 (boxed data points correspond to Figure 1). The schematic highlights the behavior of these parameters during one NW growth cycle. The lines in the data plots serve as a guide to the eye. The vertical dashed lines and the gray shading indicate bilayer step formation, i.e., a growth cycle. There is an approximately ±3° random error for the TPB angle measurements due to Fresnel fringe contrast.

fast for the VLS system to be resolved by video-rate ETEM. The consistent correlation between the filling of the rough surface *R* and rising contact angle prior to nucleation suggests the existence of a causal relationship between TPB dynamics and step formation.

4. DISCUSSION

The existence of *R* at the NW−catalyst interface can be explained, at least qualitatively, through the Wulff construction and TPB tension between the catalyst and the NW.[7,13] For ⟨111⟩-oriented NWs the anisotropic surface energy of Ge makes a single {111} plane at the liquid−solid interface energetically unfavorable. The diamond-cubic (DC) Ge interface may not necessarily assume the Wulff shape, but some degree of faceting is expected.[14] Moreover, it is known that atomically rough surfaces act as a preferential binding site prior to 2D nucleation events on crystal surfaces.[15] It is known from past literature[16] that rough surfaces in DC structures, such as Ge, grow under any

dx.doi.org/10.1021/jp1095882 |*J. Phys. Chem. C* 2011, 115, 4413–4417

finite supersaturation, $\Delta\mu$. This implies that there is no nucleation barrier for crystal growth on R's rough surface. In contrast, a planar {111} DC surface requires a considerable supersaturation to overcome a 2D nucleation barrier to form a new bilayer. These dramatically different nucleation kinetics cause R to be a temporary preferred precipitation site for dissolved Ge.

Assuming three rough surfaces are present (based on the threefold symmetry in the DC crystal structure), we estimate that filling R corresponds to approximately 2/3 the number of atoms required to form a new Ge bilayer. Such a large fraction of Ge impacts the supersaturation $\Delta\mu$ and alters the step nucleation rate during Ge NW growth. Since step propagation occurs much faster than the time resolution of the recording media, we can assume excess Ge is almost instantly precipitated into the new bilayer upon nucleation. This allows us to make two assumptions. First, the appearance of a bilayer occurs at approximately the same time as a nucleation event. Second, the liquid catalyst temporarily returns to equilibrium immediately after nucleation. Based on these assumptions, we can estimate the nucleation events by measuring the time delay between the appearance of a new Ge bilayer. To determine the time varying behavior of the supersaturation $\Delta\mu$, we employ a statistical argument based on classical nucleation theory.

The Ge NW grows via 2D nucleation and step propagation at the catalyst/NW interface. In our classical continuous picture, the free energy for a 2D Ge bilayer with N atoms can be written as[17]

$$\Delta G = \alpha N^{1/2} - \Delta\mu N \quad (1)$$

where α is a geometrically weighted coefficient for forming a new surface. The supersaturation $\Delta\mu$ is the difference between the DC and liquid Ge chemical potentials. The nucleation barrier ΔG_B (the thermal activation energy) is the maximum of eq 1.

$$\Delta G_B = \alpha^2/(4\Delta\mu) \quad (2)$$

ΔG_B is the activation energy required to form a new Ge bilayer. The size of this barrier determines the rate steps nucleate and consequently the NW growth rate. The general rate of critical nucleus formation is given by $J(t) = ZC\omega \exp(-\Delta G_B/k_bT)$ where Z is the Zeldovich factor, C is the monomer concentration, ω is molecular attachment frequency, T is temperature, and k_b is Boltzmann's constant.[18] Since a new bilayer nucleates in a supersaturated liquid alloy, the monomer concentration is a function of $\Delta\mu$ and for an ideal solution with a uniform distribution of Ge is given by $C = x = x_{eq} \exp(\Delta\mu/k_bT)$, where x is the mole fraction of Ge in the liquid and x_{eq} is the Ge equilibrium liquid mole fraction. Using eq 2 and rewriting C in terms of supersaturation, we get an expression for the nucleation rate $J(t)$ in terms of $\Delta\mu$.[17−19] Since pressure and temperature are held constant and the exponential term outgrows the pre-exponential factor,[17,18,20] we can rewrite $J(t)$ in terms of $\Delta\mu$ and three undetermined constants a, b, and c:

$$J(t) = ce^{(a\Delta\mu - b/\Delta\mu)} \quad (3)$$

The time dependence in eq 3 arises from the time varying molar Ge fraction in the catalyst $x(t)$. This gives a time varying supersaturation $\Delta\mu(x(t))$. To understand how the nucleation rate varies with time, we need to understand the dynamic behavior of $\Delta\mu$. To determine this we consider the forces acting on the TPB.

At the TPB we have a triple point force balance between solid−liquid−vapor phases at a contact angle θ_c (Figure 1A) whose value is determined by the surface energies γ_{lv}, γ_{ls}, and γ_{vs} through Young's wetting equation. The chemical potential of the NW at the TPB is locally elevated and is a function of the wetting angle θ_c.[7] The normal component of the γ_{lv} component applies a stress at the TPB, making the liquid locally more stable than the solid phase. As previously discussed, the surface of R is rough and lacks a nucleation barrier. The Gibbs free energy change ΔG_R for adding atoms to R is given by eq 1 with $\alpha = 0$

$$\Delta G_R = -\Delta\mu_R N_R \quad (4)$$

where $\Delta\mu_R$ is the local supersaturation at R and N_R is the number of atoms attached to R's equilibrium shape. $\Delta\mu_R$ is the difference between the bulk DC and liquid chemical potentials and the energy penalty associated with the stress on the facet. The stress is a function of the AuGe droplet's wetting angle θ_c and given by $\delta \sin(\theta_c)$, where δ is a positive constant including terms from the TPB contact area, atomic volume, and liquid−vapor surface energy. The force at the TPB applies a stress on the NW locally raising the chemical potential of the DC Ge atoms near the facet $\Delta\mu_R = \mu_L - (\mu_{DC} + \delta \sin(\theta_c))$.[7] Taking $\Delta\mu \equiv \mu_L - \mu_{DC}$ to be the bulk supersaturation, we get an expression for ΔG_R in terms of the TPB contact angle and $\Delta\mu$:

$$\Delta G_R = -(\Delta\mu - \delta \sin(\theta_c))N_R \quad (5)$$

The sign of ΔG_R determines whether Ge precipitates or dissolves on R. A negative ΔG_R results in Ge precipitation while a positive ΔG_R results in dissolution. Unlike the (111) DC−liquid interface, R is rough so it is both easy to attach and remove Ge atoms. In bulk phase equilibrium the chemical potentials of the DC and liquid phases are equal; i.e., $\Delta\mu = 0$. This gives $\Delta G_R = \delta \sin(\theta_c) \geq 0$ (since $\theta_c \leq 90°$) indicating at bulk equilibrium dissolution of Ge at the TPB boundary is favored. As Ge dissolves from R, the Ge concentration in the melt rises and increases the bulk supersaturation $\Delta\mu$ in the catalyst. As this occurs the contact angle relaxes, lowering θ_c as solid Ge has been removed and no longer displaces the liquid alloy. The equilibrium shape of the TPB is established when $\Delta G_R = 0$; this means the equilibrium shape of R occurs when the bulk supersaturation in the catalyst matches the stress at the TPB:

$$\Delta\mu = \delta \sin(\theta_c) \quad (6)$$

Now, suppose excess Ge is added to the alloy at equilibrium, i.e., when $\Delta G_R = 0$. This will raise $\Delta\mu$ and lead to a negative ΔG_R by eq 5 favoring Ge precipitation to R. As Ge binds to R the liquid alloy is displaced and θ_c rises. This raises the magnitude of $\delta \sin(\theta_c)$ until it matches $\Delta\mu$, pushing ΔG_R back to 0 and restoring equilibrium. As the Ge concentration varies slowly between nucleation events (~3% over 1 s), the contact angle can always match the Ge concentration. Therefore, the contact angle is an indirect measure of the Ge molar fraction and supersaturation. A high θ_c is effectively stabilized by the high Ge molar fraction in the liquid AuGe.

The steadily rising $\Delta\mu$ required to attach Ge to R also lowers the energy barrier ΔG_B for bilayer formation by eq 2, until step nucleation at the interface (Figures 1D−E). Once a new bilayer forms, the Ge molar fraction in the liquid catalyst rapidly falls approaching bulk equilibrium, pushing $\Delta\mu$ close to 0. This means $\Delta G_R \geq 0$, and dissolution of Ge from R is again favored as the high Ge molar fraction in the alloy kept $\Delta G_R = 0$ via eq 5. After relaxation, the process begins anew with the Ge molar fraction building up in the catalyst, precipitating at R and raising θ_c.

dx.doi.org/10.1021/jp1095882 |J. Phys. Chem. C 2011, 115, 4413–4417

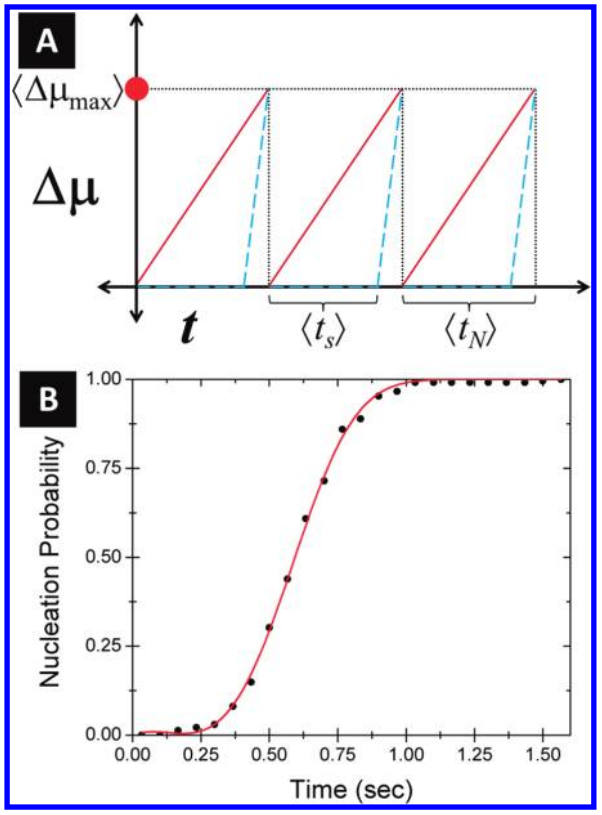

Figure 3. (A) Schematic of catalyst supersaturation $\Delta\mu$ vs time t. The red curve shows $\Delta\mu \propto t$ until nucleation occurs at $\langle\Delta\mu_{max}\rangle$. The average time required for nucleation is given by $\langle t_N\rangle$. The blue (dashed) curve shows a hypothetical behavior, where $\Delta\mu = 0$ until R is smoothed at $\langle t_s\rangle$. (B) Step nucleation probability vs time. The red curve corresponds to the fitted probability function which is a third order series expansion of the integrand in eq 8. The analysis refers to ETEM data of Ge NW growth under similar conditions as for Figure 1.

We can approximate the supersaturation as a linear function of the wetting angle $\Delta\mu \approx \delta\theta_c$. Assuming that the number of Ge atoms deposited by the decomposing digermane increases linearly with time, the precipitation of Ge onto R and θ_c will vary linearly with time, and hence $\Delta\mu \propto t$ (Figure 3A). This assumption is in agreement with our data which suggests a linearly increasing wetting angle with time preceding step nucleation (Figure 2). Since nucleation is governed by a first order rate equation, the probability of forming a single critical nucleus in time t for a system of volume V is given by an exponential sigmoidal function with a time varying rate parameter:[17]

$$P(t) = 1 - e^{-V\int_0^t J(t)\,dt} \quad (7)$$

Substituting eq 3 into eq 7 and assuming $\Delta\mu \propto t$, we get an expression for the probability of a 2D Ge bilayer nucleation event after an incubation time t:

$$P(t) = 1 - \exp\left(-c\int_0^t e^{(at - b/t)}\,dt\right) \quad (8)$$

The integrand in eq 8 can be approximated using a third order series expansion. The series expansion is performed close to the average incubation time at $t = 1$ s to avoid the singularity at $t = 0$ s. Figure 3B shows the that series expansion fits the experimental data well, further confirming that the rate of Ge bilayer formation is governed by a supersaturation that linearly increases with time.

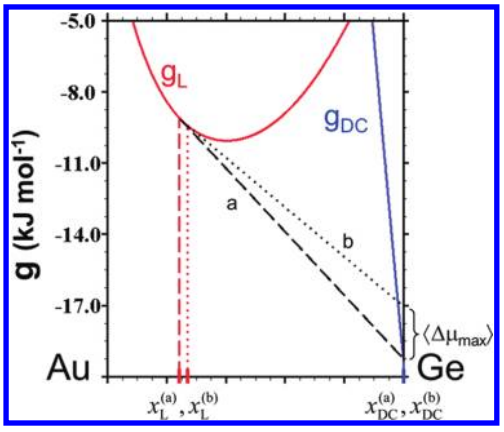

Figure 4. Calculated[22,23] molar free energies (g) of the liquid (g_L, red) and DC (g_{DC}, blue) phases at $T = 310$ °C. The average supersaturation required for Ge bilayer nucleation is $\langle\Delta\mu_{max}\rangle \approx 2000$ J mol^{-1}. Tangent "a" corresponds to the Ge molar fractions associated with bulk equilibrium between the L and DC phase. Tangent "b" corresponds to equilibrium Ge molar fractions at maximum supersaturation before nucleation. The calculated Ge molar fractions are $x_L^{(a)} = 0.243$ and $x_L^{(b)} = 0.270$.

We emphasize that $\Delta\mu \propto t$ within a growth cycle is not self-evident. As shown in Figure 3A, one could alternatively expect the presence of R to temporarily stabilize the Ge molar fraction and keep $\Delta\mu = 0$ in the melt. $\Delta\mu$ would only start to rise after R smoothes, i.e., when the catalyst−NW interface consists of a single liquid−solid (111) interface at time $\langle t_s\rangle$ (Figure 3A). However, this is inconsistent with our experimental data, in particular the incomplete filling of R before bilayer nucleation (Figure 1D). The continuously rising Ge supersaturation we find instead is a consequence of the finite $\Delta\mu$ needed for precipitation on R which gets progressively larger as θ_c rises via eq 6.

The magnitude of the average maximum supersaturation required to initiate a 2D nucleation event, $\langle\Delta\mu_{max}\rangle$, is important as it controls the rate of bilayer nucleation and NW kinking.[21] Although normally difficult to quantify, our ETEM data here allows a reasonable estimate of the magnitude of $\langle\Delta\mu_{max}\rangle$. Assuming the NW in Figure 1 has a hexagonal cross section and the catalyst is hemispherical, we can estimate the number of Ge atoms in the bilayer to be approximately 6700. Since 2/3 of the Ge atoms needed to form a bilayer go into R, the remaining 1/3 raise the Ge molar fraction in the catalyst by 3%. Using the calculated[22,23] free energy functions for the AuGe system, a 3% increase in the Ge mole fractions gives $\langle\Delta\mu_{max}\rangle \approx 2000$ J mol^{-1} at 310 °C, Figure 4. Note that changes in the supersaturation caused by the Gibbs−Thompson effect are assumed to be small as the catalyst diameter is relatively large (≈ 27 nm).[24]

5. CONCLUSIONS

We show that a growth cycle for VLS-based NW growth, i.e., the period for the addition of a new NW layer at the catalyst interface, is dictated by the presence of atomically rough surfaces around the TPB. A NW growth cycle starts by preferential Ge precipitation at the rough TPB area, which increases the wetting angle of the liquid catalyst. The supersaturation of the catalyst thereby continuously increases with time to accommodate both the steady precursor decomposition and the rising wetting angle. As the supersaturation continues to rise, the kinetic barrier for the

formation of a new NW bilayer layer falls until step nucleation occurs. Subsequent step flow rapidly lowers the catalyst supersaturation which leads to the partial dissolution of the Ge in the TPB area and completes the growth cycle.

Our arguments have been general and based on few system specific assumptions. Thus, our model may be applicable to other catalytically grown NWs and relevant for understanding liquid−solid interface propagation in dimensionally confined systems. Furthermore, since the equilibrium contact angle is governed by Young's wetting equation, the relative magnitude of TPB stress is partly controlled by surface energy differences of the vapor, solid, and liquid phases. Our findings suggest that changing the surface energetics of the system, for instance, through the addition of dopant gases during the CVD process, alters the kinetics of NW growth. Understanding the TPB behavior and local interfacial dynamics will allow for greater control over NW growth.

■ ASSOCIATED CONTENT

Supporting Information. Bright-field ETEM video of Ge NW growth from a liquid AuGe catalyst particle at $T \approx 310$ °C in Ge_2H_6 (30 % in He) at $\approx 4 \times 10^{-3}$ mbar total pressure. This material is available free of charge via the Internet at http://pubs.acs.org.

■ AUTHOR INFORMATION

Corresponding Author
*E-mail sh315@cam.ac.uk.

■ ACKNOWLEDGMENT

A.D.G. acknowledges funding from the Marshall Aid Commemoration Commission. C.D. and S.H. acknowledges funding from the Royal Society. We gratefully acknowledge helpful discussions and microscopy assistance provided by Renu Sharma. We gratefully acknowledge the use of facilities within the LeRoy Eyring Center for Solid State Science at Arizona State University.

■ REFERENCES

(1) Hiruma, K.; Yazawa, M.; Katsuyama, T.; Ogawa, K.; Haraguchi, K.; Koguchi, M.; Kakibayashi, H. *J. Appl. Phys.* **1995**, *77*, 447.
(2) Li, Y.; Qian, F.; Xiang, J.; Lieber, C. M. *Mater. Today* **2006**, *9*, 18.
(3) Wagner, R. S.; Ellis, W. C. *Appl. Phys. Lett.* **1964**, *4*, 89.
(4) Hofmann, S.; Sharma, R.; Wirth, C. T.; Cervantes-Sodi, F.; Ducati, C.; Kasama, T.; Dunin-Borkowski, R. E.; Drucker, J.; Bennett, P.; Robertson, J. *Nat. Mater.* **2008**, *7*, 2008.
(5) Wen, C. Y.; Reuter, M. C.; Bruley, J.; Tersoff, J.; Kodambaka, S.; Stach, E. A.; Ross, F. M. *Science* **2009**, *326*, 1247.
(6) Glas, F.; Harmand, J.-C.; Patriarche, G. *Phys. Rev. Lett.* **2010**, *104*, 135501.
(7) Schwarz, K. W.; Tersoff, J. *Phys. Rev. Lett.* **2009**, *102*, 206101.
(8) Dayeh, S. A.; Picraux, S. T. *Nano Lett.* **2010**, *10*, 4032.
(9) Wallentin, J.; Ek, M.; Wallenberg, L. R.; Samuelson, L.; Deppert, K.; Borgström, M. T. *Nano Lett.* **2010**, *10*, 4807.
(10) Oh, S. H.; Chisholm, M. F.; Kauffmann, Y.; Kaplan, W. D.; Luo, W.; Ruhle, M.; Scheu, C. *Science* **2010**, *330*, 489.
(11) Utke, I.; Hoffmann, P.; Melngailis, J. *J. Vac. Sci. Technol., B* **2008**, *26*, 1197.
(12) Gamalski, A. D.; Tersoff, J.; Sharma, R.; Ducati, C.; Hofmann, S. *Nano Lett.* **2010**, *10*, 2972.
(13) Stekolnikov, A. A.; Bechstedt, F. *Phys. Rev. B* **2005**, *72*, 125326.
(14) Haxhimali, T.; Buta, D.; Asta, M.; Voorhees, P. W.; Hoyt, J. J. *Phys. Rev. E* **2009**, *80*, 500601.
(15) Tersoff, J.; Gon, A. W. D. v. d.; Tromp, R. M. *Phys. Rev. Lett.* **1993**, *70*, 1143.
(16) Battaile, C. C.; Srolovitz, D. J.; Butler, J. E. *Diamond Relat. Mater.* **1997**, *6*, 1198.
(17) Kashchiev, D. *Nucleation*; Butterworth-Heinemann: Burlington, MA, 2000.
(18) Turnbull, D.; Fisher, J. C. *J. Chem. Phys.* **1949**, *17*, 71.
(19) Wacaser, B. A.; Dick, K. A.; Johansson, J.; Borgström, M. T.; Deppert, K.; Samuelson, L. *Adv. Mater.* **2009**, *21*, 153.
(20) Markov, I. V. *Crystal Growth for Beginners*; World Scientific Publishing: Hackensack, NJ, 2003.
(21) Madras, P.; Dailey, E.; Drucker, J. *Nano Lett.* **2009**, *9*, 3826.
(22) Chevalier, P. Y. *Thermochim. Acta* **1989**, *141*, 217.
(23) Almazouzi, A.; Bernardini, J.; Moya, E. G.; Bracht, H.; Stolwijk, N. A.; Mehrer, H. *J. Appl. Phys.* **1991**, *70*, 1345.
(24) Schwalback, E. J.; Voorhees, P. W. *Nano Lett.* **2008**, *8*, 3739.